The Hubbard model description of the TCNQ related singular features in photoemission of TTF-TCNQ

2006 J. Phys.: Condens. Matter 18 5191

(http://iopscience.iop.org/0953-8984/18/22/019)

INSTITUTE OF PHYSICS PUBLISHING JOURNAL OF PHYSICS: CONDENSED MATTER

J. Phys.: Condens. Matter **18** (2006) 5191–5212 doi:10.1088/0953-8984/18/22/019

The Hubbard model description of the TCNQ related singular features in photoemission of TTF-TCNQ

J M P Carmelo[1,2], K Penc[3], P D Sacramento[4], M Sing[5] and R Claessen[5]

[1] GCEP-Center of Physics, University of Minho, Campus Gualtar, P-4710-057, Braga, Portugal
[2] Department of Physics, Massachusetts Institute of Technology, Cambridge, MA 02139-4307, USA
[3] Research Institute for Solid State Physics and Optics, H-1525 Budapest, PO Box 49, Hungary
[4] Departamento de Física and CFIF, Instituto Superior Técnico, P-1049-001 Lisboa, Portugal
[5] Experimentelle Physik 4, Universität Würzburg Am Hubland, D-97074, Würzburg, Germany

Received 9 February 2006, in final form 19 April 2006
Published 19 May 2006
Online at stacks.iop.org/JPhysCM/18/5191

Abstract

In this paper we use the pseudofermion dynamical theory (PDT) to study the singular spectral features due to one-electron removal within the one-dimensional Hubbard model. The PDT reveals that in the whole (k, ω)-plane such features are of the power-law type and correspond to well defined lines of three types: charge singular branch lines, spin singular branch lines and border lines. One of our goals is the study of the momentum and energy dependence of the distribution of the spectral weight in the vicinity of such lines. We find that the charge and spin branch lines correspond to the main tetracyanoquinodimethane (TCNQ) peak dispersions observed with angle-resolved photoelectron spectroscopy in the quasi-1D organic conductor tetrathiafulvalene-tetracyanoquinodimethane (TTF-TCNQ). Our expressions refer to all values of the electronic density and on-site repulsion U. The weight distribution in the vicinity of the singular spectral lines is fully controlled by the overall pseudofermion phase shifts. Moreover, the shape of these lines is determined by the bare-momentum dependence of the pseudofermion energy dispersions.

1. Introduction

Early studies of quasi-one-dimensional (1D) compounds have focused on the various low-energy phases which are not metallic and correspond to broken-symmetry states [1, 2]. Recently, the resolution of photoemission experiments has improved, and the *normal* state of these compounds was found to display exotic spectral properties [3–5]. Study of the microscopic mechanisms behind such properties has until now remained an interesting open problem. Indeed, the finite-energy spectral dispersions recently observed in such metals by angle-resolved photoelectron spectroscopy (ARPES) reveal significant discrepancies from the conventional band-structure description [1, 3–5].

There is some evidence that the 1D Hubbard model [6, 7] successfully describes the transport properties and other exotic properties observed in some low-dimensional materials [8] and that the electronic correlation effects described by the model could contain the finite-energy microscopic mechanisms [3, 4] that control the above finite-energy spectral properties. Until recently very little was known about the finite-energy spectral properties of that model for finite values of the on-site repulsion U. This is in contrast to simpler models [9]. Indeed, the usual techniques such as bosonization [10] and conformal-field theory [11–19] are very useful for the study of the Tomanaga–Luttinger liquid (TLL) low-energy regimen but do not apply at finite energy. Valuable qualitative information can be obtained for $U \rightarrow \infty$ by use of the method of [20, 21]. However, a quantitative description of the finite-energy spectral properties of quasi-1D metals requires the solution of the problem for finite values of the on-site Coulombian repulsion U. The method of [22] refers to features of the insulator phase. For $U \approx 4t$, where t is the transfer integral, there are numerical results for the one-electron spectral function [23]. Unfortunately, the latter results provide very little information about the microscopic mechanisms behind the finite-energy spectral properties.

Recently, the preliminary use of the finite-energy holon and spinon representation introduced in [24] and further studied in [25] and the related pseudofermion description of [26–29], revealed that most singular features of the one-electron-removal spectral function correspond to separate charge and spin branch lines [3, 4]. Interestingly, the singular branch lines associated with the one-electron-removal spectral function show quantitative agreement with the tetracyanoquinodimethane (TCNQ) peak dispersions observed by ARPES in the quasi-1D organic conductor tetrathiafulvalene-tetracyanoquinodimethane (TTF-TCNQ) [3–5]. However, these studies provide no information about the momentum and energy dependence of the spectral-weight distribution in the vicinity of the charge and spin branch lines. A preliminary study of that dependence was recently presented in short form in [30]. Thereafter a study of the same problem by means of the dynamical density matrix renormalization group (DDMRG) method led to very similar results [31].

The main goal of this paper is the extension of the preliminary results presented in [30]. Our investigation relies on the pseudofermion dynamical theory (PDT) introduced in [26]. Such a theory provides the general finite-energy spectral-weight distributions for the metallic phase of the model (1) for all values of energy and momentum. However, the amount of one-electron-removal weight in regions away from the singular spectral lines is small. Therefore, we limit our studies here to the vicinity of such lines. Our investigation focuses on the one-electron-removal spectral function for all values of U and electronic density in the vicinity of the singular charge and spin branch lines, which turn out to be the most important spectral features for the description of the unusual TCNQ photoemission spectral lines. The evaluation of the small spectral-weight distributions away from the singular spectral features considered here requires the use of involved numerical calculations which will be carried out elsewhere.

The pseudofermion description refers to the *pseudofermion subspace* (PS) [26]. The one-electron-removal excitations studied in this paper are contained in such a Hilbert subspace. The PDT refers to all energy scales but in the limit of low energy leads to the known conformal-field-theory spectral-function and correlated-function expressions [27]. In [32] the PDT is combined with the renormalization group for the study of the microscopic mechanisms behind the phase diagram observed in the $(TMTTF)_2X$ and $(TMTSF)_2X$ series of quasi-1D organic compounds. These studies are consistent with the latter phase diagram and explain why there are no superconducting phases in TTF-TCNQ. The PDT used in this paper in the study of the one-electron-removal spectral function of the 1D Hubbard model applies to related integrable interacting problems [33] and therefore has wide applicability.

The paper is organized as follows. In section 2 we introduce the one-electron-removal spectral-function problem, the 1D Hubbard model, and some basic information about the pseudofermion description. The introduction to the PDT and of the corresponding general spectral-function expressions used in our investigation is the subject of section 3. Section 4 is devoted to the the study of the weight distributions for one-electron removal. Moreover, we investigate the limiting behaviour of the spectral function in the vicinity of the branch lines both for $U/t \rightarrow 0$ and $U/t \rightarrow \infty$. Discussion of the relation of our theoretical predictions to the TCNQ branch lines observed by angle-resolved photoelectron spectroscopy in the quasi-1D organic compound TTF-TCNQ and concluding remarks are presented in section 5.

2. The problem and the pseudofermion description

2.1. The model and the one-electron-removal spectral functions

The 1D Hubbard model reads,

$$\hat{H} = -t \sum_{j,\sigma} [c^{\dagger}_{j,\sigma} c_{j+1,\sigma} + \text{h.c.}] + U \sum_{j} \hat{n}_{j,\uparrow} \hat{n}_{j,\downarrow}, \tag{1}$$

where $c^{\dagger}_{j,\sigma}$ and $c_{j,\sigma}$ are spin-projection $\sigma = \uparrow, \downarrow$ electron operators at site $j = 1, 2, \ldots, N_a$ and $\hat{n}_{j,\sigma} = c^{\dagger}_{j,\sigma} c_{j,\sigma}$. The model (1) describes $N_{\uparrow}$ spin-up electrons and $N_{\downarrow}$ spin-down electrons in a chain of N_a sites. We denote the electronic number by $N = N_{\uparrow} + N_{\downarrow}$. The number of lattice sites N_a is even and very large. For simplicity, we use units such that both the lattice spacing and the Planck constant are one. In these units the chain length L is such that $L = N_a$. Our results refer to periodic boundary conditions. We consider an electronic density $n = n_{\uparrow} + n_{\downarrow}$ in the range $0 < n < 1$ and a spin density $m = n_{\uparrow} - n_{\downarrow}$ such that $m \rightarrow 0$, where $n_{\sigma} = N_{\sigma}/L$ and $\sigma = \uparrow, \downarrow$. However, the calculations are performed for finite values of the spin density m. For $U/t > 0$ the limit $m \rightarrow 0$ is taken in the end of the calculation and leads to the correct $m = 0$ results. The Fermi momentum is $k_{\rm F} = \pi n/2$ and the electronic charge reads $-e$.

The one-electron-removal spectral function $B(k, \omega)$ is given by,

$$B(k, \omega) = \sum_{\sigma} \sum_{f} |\langle f | c_{k,\sigma} | \text{GS} \rangle|^2 \delta\Big(\omega + E_f - E_{\rm GS}\Big), \qquad \omega < 0. \tag{2}$$

Here $c_{k,\sigma}$ is an electron annihilation operator of momentum k and $|\text{GS}\rangle$ denotes the initial N-electron ground state. The f summation runs over the $N-1$-electron excited energy eigenstates and $[E_f - E_{\rm GS}]$ are the corresponding excitation energies. We use an extended momentum scheme such that $k \in (-\infty, +\infty)$ for the expression given in equation (2), yet it is a simple exercise to obtain the corresponding spectral function expression for the first Brillouin zone.

2.2. The pseudofermion description

We now proceed to summarize the pseudofermion description of the excitation spectrum [24–29]. It is closely related to the holons and spinons as defined in [24]. Here we use the designations $\pm 1/2$ holons and $\pm 1/2$ spinons in terms of the η-spin and spin projections, respectively. Such objects are well defined occupancy configurations of rotated electrons, which are related to the original electrons by a unitary transformation [24]. The holons (and spinons) have η-spin $1/2$, with η-spin projection $\pm 1/2$, and spin zero (and spin $1/2$, with spin projection $\pm 1/2$, and no charge degrees of freedom), and are defined so that the rotated-electron double occupation content equals the number of $-1/2$ holons. Starting from a given ground state, the pseudofermion subspace (PS) is spanned by the excited energy eigenstates that can be described in terms of occupancy configurations of pseudofermions, Yang holons and HL spinons. The one- and two-electron excitations are contained in the PS [26, 27].

The $c0$ pseudofermions have no spin and η-spin degrees of freedom. The $c\nu$ pseudofermions for $\nu > 0$ (and $s\nu$ pseudofermions), are composite objects having η-spin zero (and spin zero) consisting of an equal number $\nu = 1, 2, \ldots$ of $-1/2$ holons and $+1/2$ holons (and $-1/2$ spinons and $+1/2$ spinons). In this paper we use the notation $\alpha\nu$ pseudofermion, where $\alpha = c, s$ and $\nu = 0, 1, 2, \ldots$ for the $c\nu$ branches and $\nu = 1, 2, \ldots$ for the $s\nu$ branches. The holons, $c0$ pseudofermions and composite $c\nu$ pseudofermions are charged objects. The different pseudofermion branches correspond to well known types of Bethe ansatz (BA) excitations. For instance, in the PS the $c0$ pseudofermion occupancy configurations describe the BA charge distribution of excitations of k and those of the $c\nu$ pseudofermions for $\nu > 0$ (and $s\nu$ pseudofermions) describe the BA charge string excitations of length ν (and BA spin string excitations of length ν) [7].

The properties of the Yang holons and HL spinons follow from the invariance of the three generators of the η-spin $SU(2)$ algebra and three generators of the spin $SU(2)$ algebra, respectively, under the electron–rotated-electron unitary transformation. Indeed, the Yang holons and HL spinons are also invariant under that transformation [24]. Therefore, the operators that transform such objects have the same form in terms of electron and rotated-electron creation and annihilation operators. For instance, the η-spin off-diagonal generator that creates (and annihilates) an on-site electronic Cooper pair, equation (7) of [24], transforms a $+1/2$ Yang holon (and a $-1/2$ Yang holon) into a $-1/2$ Yang holon (and a $+1/2$ Yang holon). Furthermore, the spin off-diagonal generator that flips an on-site electronic up spin (and down spin) onto an on-site electronic down spin (and up spin), equation (8) of [24], also transforms a $+1/2$ HL spinon (and a $-1/2$ HL spinon) into a $-1/2$ HL spinon (and a $+1/2$ HL spinon). Thus, the occupancies of these objects involving Yang holons with different η-spin projections $+1/2$ and $-1/2$ and/or HL spinons with different spin projections $+1/2$ and $-1/2$ describe the energy eigenstates that are not contained the BA solution. The corresponding energy eigenstates contained in that solution have precisely the same pseudofermion occupancy configurations and the same Yang holon and HL spinon total numbers. However, all the Yang holons and HL spinons of the latter states have the same η-spin and spin projections, respectively. (For more information about Yang holons and HL spinons see section 2.4 of [24].)

We denote the number of $\alpha\nu$ pseudofermions by $N_{\alpha\nu}$ and the number of $\pm 1/2$ Yang holons ($\alpha = c$) and $\pm 1/2$ HL spinons ($\alpha = s$) by $L_{\alpha,\pm 1/2}$. As mentioned above, besides corresponding to well defined occupancies of the BA quantum numbers, the holons, spinons and pseudofermions can also be expressed in terms of rotated electrons. For instance, N_{c0} equals the number of rotated-electron singly occupied sites and $[N_a - N_{c0}]$ equals the number of rotated-electron doubly occupied plus unoccupied sites. We call $M_{\alpha,\pm 1/2}$ the number of $\pm 1/2$ holons ($\alpha = c$) and $\pm 1/2$ spinons ($\alpha = s$). The latter number and that of $\pm 1/2$ Yang holons ($\alpha = c$) and $\pm 1/2$ HL spinons ($\alpha = s$) are given by $M_{\alpha,\pm 1/2} = L_{\alpha,\pm 1/2} + \sum_{\nu=1}^{\infty} \nu N_{\alpha\nu}$ and $L_{\alpha,\pm 1/2} = S_\alpha \mp S^z_\alpha$, respectively. Here S_c (and S_s) denotes the η-spin (and spin) of a state and S^z_c (and S^z_s) its η-spin (and spin) projection. (See equation (2) of [24].)

Within the pseudofermion, Yang holon and HL spinon description the energy and momentum spectrum of the PS energy eigenstates has the form provided in equations (28)–(34) of [26]. Such a spectrum is expressed in terms of the pseudofermion energy dispersions defined in equations (C.15)–(C.18) of [24], pseudofermion bare-momentum distribution-function deviations given in equations (13)–(17) of [26] and Yang holon ($\alpha = c$) and HL spinon ($\alpha = s$) occupancies $L_{\alpha,\pm 1/2} = S_\alpha \mp S^z_\alpha$

Fortunately, for densities $0 < n < 1$ and $m \to 0$ only the charge $c0$ and spin $s1$ pseudofermion branches contribute to the one-electron-removal dominant processes considered in this paper. Indeed, the one-electron-removal excitations have nearly no overlap with excited

energy eigenstates with finite occupancies of $-1/2$ Yang holons, $-1/2$ HL spinons and $c\nu$ and $s\nu'$ pseudofermions such that $\nu \geqslant 1$ and $\nu' \geqslant 2$, respectively.

An important point of the PDT is that the pseudofermions or pseudofermion holes created under each ground-state–excited-state transition play the role of the scattering centres of the theory [28, 29]. The wavefunctions of all pseudofermions and holes whose occupancy configurations describe the excited states feel the creation of such objects through the corresponding two-pseudofermion phase shifts. The spectral-weight distributions are fully controlled by such two-pseudofermion quantities [26, 27]. The main technical problem concerning the evaluation of the spectral-weight distributions by the PDT is that the overall pseudofermion phase shifts resulting from the two-particle events have a functional character, since their values are different for each excited state. The relation of the overall pseudofermion phase shifts to the conventional phase shifts considered previously in the literature of the 1D Hubbard model was recently clarified in the second paper of [29]: the studies in that paper reveal that the overall pseudofermion phase shift given below is a generalization of the conventional phase shifts considered previously and that it is the most suitable for applications to the finite-energy spectral properties studied here.

Most of our final expressions refer to densities $0 < n < 1$ and $m \rightarrow 0$. According to the above general analysis, the charge $c0$ pseudofermion is a spin-less and η-spin-less object that carries charge $-e$, and the spin $s1$ pseudofermion is a charge-less and spin-zero two-spinon composite object. The $\alpha\nu = c0, s1$ pseudofermions carry canonical-momentum $\bar{q} = q + Q^{\Phi}_{\alpha\nu}(q)/L$. Here q is the *bare-momentum* and $Q^{\Phi}_{\alpha\nu}(q)/2$ is the overall scattering phase shift given by [28]

$$Q^{\Phi}_{\alpha\nu}(q)/2 = \sum_{\alpha'\nu'=c0,s1} \sum_{q'} \pi \Phi_{\alpha\nu,\alpha'\nu'}(q,q')\Delta N_{\alpha'\nu'}(q'); \qquad \alpha\nu = c0, s1. \tag{3}$$

On the right-hand side of this equation $\Delta N_{\alpha\nu}(q) = \Delta\mathcal{N}_{\alpha\nu}(\bar{q})$ is the bare-momentum distribution function deviation $\Delta N_{\alpha\nu}(q) = N_{\alpha\nu}(q) - N^0_{\alpha\nu}(q)$ and the elementary two-pseudofermion phase shifts $\Phi_{\alpha\nu,\alpha'\nu'}(q,q')$ in units of π are such that $+\pi\Phi_{\alpha\nu,\alpha'\nu'}(q,q')$ (and $-\pi\Phi_{\alpha\nu,\alpha'\nu'}(q,q')$) gives the phase shift acquired by the bare-momentum $q\alpha\nu$ pseudofermion or hole wavefunction when such an object is scattered by a bare-momentum $q'\alpha'\nu'$ pseudofermion (and $\alpha'\nu'$ pseudofermion hole) created under a ground-state–excited-energy-eigenstate transition [28]. The bare-momentum distribution-function deviations $\Delta N_{\alpha'\nu'}(q')$ of equation (3) result from such a transition. In expression (3) these deviations refer to the $c0$ and $s1$ branches only and thus describe excited energy eigenstates generated by one-electron-removal dominant processes. The corresponding general expression is given in equation (2) of [28] and involves summations over all pseudofermion branches.

Although the $\alpha\nu$ pseudoparticles carry bare-momentum q [24, 25], one can also label the corresponding $\alpha\nu$ pseudofermions by that bare-momentum. Indeed, the latter pseudofermions carry canonical-momentum $\bar{q} = q + Q^{\Phi}_{\alpha\nu}(q)/L$, but this latter expression provides an one-to-one relation between the bare-momentum q and the canonical-momentum $\bar{q}$. The pseudoparticles have residual-interaction energy terms which do not allow the expression of the electronic spectral functions as a convolution of $\alpha\nu$ pseudoparticle spectral functions [26]. A property which plays a central role in the PDT is that for the corresponding $\alpha\nu$ pseudofermions, such residual-interaction energy terms are exactly cancelled by the overall scattering phase shift $Q^{\Phi}_{\alpha\nu}(q)/2$. By cancelling the residual interactions exactly, the associated canonical-momentum shift $Q^{\Phi}_{\alpha\nu}(q)/L$ transfers the information recorded in these interactions over to the pseudofermion canonical-momentum.

The overall $\alpha\nu$ pseudofermion or $\alpha\nu$ pseudofermion hole phase shift acquired under a ground-state–excited-energy-eigenstate transition is given by $Q_{\alpha\nu}(q)/2 = Q^0_{\alpha\nu}/2 + Q^{\Phi}_{\alpha\nu}(q)/2$ [28, 29]. Here $Q^{\Phi}_{\alpha\nu}(q)/2$ is provided in equation (3) and $Q^0_{\alpha\nu}/2 = 0, \pm\pi/2$ is

an overall $\alpha\nu$ pseudoparticle or hole scatterer-less phase shift whose value is well defined for each excitation subspace spanned by energy eigenstates with the same pseudofermion numbers [26, 28]. It is such that under a ground-state–excited-energy-eigenstate transition the $\alpha\nu$ pseudoparticle and hole discrete bare-momentum value q_j is shifted by $Q^0_{\alpha\nu}(q_j)/L$. The overall phase shift $Q_{\alpha\nu}(q)/2$ leads to a corresponding canonical-momentum shift $Q_{\alpha\nu}(q_j)/L$ for the discrete canonical-momentum values of the $\alpha\nu$ pseudofermions and holes. The structure of the overall scattering phase shift (3) confirms that its value is different for each excited state. Indeed, the bare-momentum distribution function deviation $\Delta N_{\alpha\nu}(q) = N_{\alpha\nu}(q) - N^0_{\alpha\nu}(q)$ has a well defined value for each energy eigenstate. In turn, for given values of the densities, U/t, scatterer bare-momentum q and scattering-centre bare-momentum q' the value of the two-pseudofermion phase shift $\pi\Phi_{\alpha\nu,\alpha'\nu'}(q,q')$ is universal and equal for all excited states. The density, interaction and momentum dependence of such a two-pseudofermion phase shift is studied in detail in the first paper of [29].

Note that for each $\alpha\nu$ branch the continuum bare-momentum q corresponds to a set of discrete bare-momentum values q_j such that $q_{j+1} - q_j = 2\pi/L$. Here $j = 1, 2, \ldots, N^*_{\alpha\nu}$ and the number $N^*_{\alpha\nu} = N_{\alpha\nu} + N^{\rm h}_{\alpha\nu}$ is given in equations (B6)–(B8) and (B11) of [24]. $N_{\alpha\nu}$ and $N^{\rm h}_{\alpha\nu}$ denote the number of $\alpha\nu$ pseudofermions and $\alpha\nu$ pseudofermion holes, respectively. $N^*_{\alpha\nu}$ equals the number of sites of the effective $\alpha\nu$ lattice [28], which plays an important role in the pseudoparticle and pseudofermion descriptions. For the $\alpha\nu = c0, s1$ branches the number $N^{\rm h}_{\alpha\nu}$ reads

$$N^{\rm h}_{c0} = [N_a - N_{c0}]; \qquad N^{\rm h}_{s1} = N_{c0} - 2\sum_{\nu'=1}^{\infty} N_{s\nu'}, \tag{4}$$

where in our case $N^{\rm h}_{s1} = N_{c0} - 2N_{s1}$. We used equation (B.11) of [24] to derive the expression given in equation (4) for $N^{\rm h}_{s1}$, such that $N^{\rm h}_{s1} = 0$ for the $m \to 0$ initial ground state.

The pseudofermion occupancy configurations of the effective $\alpha\nu$ lattices correspond to well defined occupancy configurations of the original lattice by rotated electrons, which are related to electrons by a unitary transformation [24, 25]. However, while in terms of the electrons the quantum problem is strongly interacting and non-perturbative, in terms of pseudofermions there are only two-particle zero-momentum forward-scattering events associated with the overall scattering phase-shift functional (3).

As the quasi-particles of Fermi liquid theory have momentum-dependent energy dispersions, the charge and spin pseudofermions also have energy bands $\epsilon_{c0}(q)$ and $\epsilon_{s1}(q)$ such that $|q| \leqslant \pi$ and $|q| \leqslant k_{\rm F}$, respectively. These energy dispersions are plotted in figures 6 and 7 of [25]. (As mentioned above, they are defined by equations (C.15) and (C.16) of [24], respectively.) Also the group velocity $v_{\alpha\nu}(q) = \partial\epsilon_{\alpha\nu}(q)/\partial q$ and the *Fermi-point* velocity $v_{\alpha\nu} \equiv v_{\alpha\nu}(q^0_{{\rm F}\alpha\nu})$ appear in the spectral-function expressions. Here $q^0_{{\rm F}c0} = 2k_{\rm F}$ and $q^0_{{\rm F}s1} = k_{{\rm F}\downarrow} = k_{\rm F}$ as $m \to 0$ define the ground-state *Fermi points* [24, 26]. In section 4 we confirm that the pseudofermion energy bands fully determine the shape of the one-electron-removal spectral function in the proximity of the branch lines studied in that section. In the ground state the $s1$ pseudofermion band is filled and the $c0$ pseudofermions occupy the bare-momentum domain $0 \leqslant |q| \leqslant 2k_{\rm F}$ (leaving $2k_{\rm F} < |q| \leqslant \pi$ empty).

3. The general spectral-function expressions used in our study

3.1. PDT dominant processes

The one-electron-removal problem studied in this paper involves only the PDT dominant processes. The dominant (and non-dominant) processes correspond to the $i = 0$ (and $i > 0$)

terms on the right-hand side of the general spectral-function expression given in equation (41) of the first paper of [26]. Furthermore, only such dominant processes contribute to the one-electron-removal spectral-function power-law expressions obtained in this paper. The initial ground state and excited energy eigenstates of equation (2) that are associated with the one-electron-removal dominant processes can be expressed in terms of occupancy configurations of the $c0$ and $s1$ pseudofermions. For one-electron removal, the dominant processes involve creation of one pseudofermion hole in both the bands $\epsilon_{c0}(q)$ and $\epsilon_{s1}(q)$. In addition to small-momentum and low-energy $c0$ and $s1$ pseudofermion particle–hole processes, which conserve the pseudofermion numbers, the dominant processes involve creation of one $c0$ pseudofermion hole and one $s1$ pseudofermion hole at bare-momentum values q and q', respectively. Thus, the excited energy eigenstates generated by these one-electron-removal dominant processes belong to subspaces whose $c0$ pseudofermion and $s1$ pseudofermion hole number ground-state deviations are given by

$$\Delta N^{\rm h}_{c0} = -\Delta N_{c0} = 1; \qquad \Delta N^{\rm h}_{s1} = 1. \tag{5}$$

Moreover, as discussed in sections 4 and 5, the main one-electron-removal spectral-function singular features are associated with the charge $c0$ and spin $s1$ pseudofermion branch lines.

The domain of the (k,ω)-plane whose spectral weight is generated by one-electron-removal dominant processes is contained in the region of negative ω/t values of figure 1 of [30]. (That figure uses the extended momentum scheme also used here.) Such a domain is limited above by the s line for momentum values between $k=0$ and $k=k_{\rm F}$, the c'' line from $k=k_{\rm F}$ until that line reaches the c' line at $k=2k_{\rm F}$, the c' line from the momentum $k=2k_{\rm F}$ until $k=3k_{\rm F}$ and the s line between the momentum values $k=3k_{\rm F}$ and $k=5k_{\rm F}$. The same domain is limited below by the lowest line of the figure.

When both the bare-momentum values q and q' of the two created pseudofermion holes are away from the *Fermi points* and such that $v_{c0}(q) \neq v_{s1}(q')$, the corresponding dominant processes do not lead to singular spectral features and generate the one-electron-removal spectral weight for (k,ω)-plane regions away from these features. Since the latter weight is small, in this paper we do not study its intensity distribution in the (k,ω)-plane. A first type of singular feature corresponds to lines generated by such processes where both created objects move with the same group velocity, $v_{c0}(q) = v_{s1}(q')$, and the spectral feature corresponds to a border line, $\omega = \omega_{\rm BL}(k) = [\pm\epsilon_{c0}(q) - \epsilon_{1s}(q')]\delta_{v_{c0}(q),v_{s1}(q')}$, in the (k,ω)-plane. In this case the spectral function reads

$$B(k,\omega) \approx C_{\rm BL}(k)(\omega - \omega_{\rm BL}(k))^{-1/2}, \tag{6}$$

in the vicinity and just above such a line. However, as discussed in section 5, for the TCNQ-related spectral features the only existing border line for the density of the TCNQ stacks of molecules of TTF-TCNQ leads to a weak feature mentioned in section 5, which we do not study in section 4.

The second type of spectral feature corresponds to the branch lines studied in this paper, such that either q or q' equals one of the corresponding pseudofermion branch *Fermi points*. Thus, such features are generated by processes where a $\alpha\nu$ pseudofermion hole is created for all the available values of bare-momentum q and a second $\alpha'\nu'$ pseudofermion hole is created at one of its two *Fermi points* $\pm q^0_{{\rm F}\alpha'\nu'}$, where $\alpha\nu = c0, s1$ and $\alpha'\nu' = s1, c0$, respectively.

For densities $0 < n < 1$ and $0 < m < n$ the $\alpha\nu = c0, s1$ pseudofermion phase-shift-related functional

$$2\Delta^{\iota}_{\alpha\nu} = \left(\iota\Delta N^{0,{\rm F}}_{\alpha\nu,\iota} + \frac{Q_{\alpha\nu}(\iota q^0_{{\rm F}\alpha\nu})}{2\pi}\right)^2 = \left(\iota\Delta N^{\rm F}_{\alpha\nu,\iota} + \frac{Q^{\Phi}_{\alpha\nu}(\iota q^0_{{\rm F}\alpha\nu})}{2\pi}\right)^2, \tag{7}$$

where $\iota = \pm 1$ and $\alpha\nu = c0, s1$, controls the exponents of the spectral-function power-law expressions in the vicinity of the charge and spin branch lines [26]. Here $\Delta N^{\rm F}_{\alpha\nu,\iota}$ is the

deviation in the number of $\alpha\nu = c0, s1$ pseudofermions at the *Fermi points* and $Q^{\Phi}(\iota q^0_{F\alpha\nu})/2$ and $Q_{\alpha\nu}(\iota q^0_{F\alpha\nu})/2 = Q^0_{\alpha\nu}/2 + Q^{\Phi}(\iota q^0_{F\alpha\nu})/2$ are the overall scattering and the overall phase shifts, respectively, of $\alpha\nu$ pseudofermion or hole scatterers at the bare-momentum *Fermi values* $\iota q^0_{F\alpha\nu} = \pm q^0_{F\alpha\nu}$. Note that the deviation $\Delta N^F_{\alpha\nu,\iota} = \iota\Delta N^{0,F}_{\alpha\nu,\iota} + Q^0_{\alpha\nu}/2\pi$ involves both contributions from the scatterer-less overall phase shift $Q^0_{\alpha\nu}/2$ and the number deviation $\Delta N^{0,F}_{\alpha\nu,\iota}$ generated by the creation or annihilation pseudofermion processes at the *Fermi points*. We also consider the $\alpha\nu = c0, s1$ current number deviation $2\Delta J^F_{\alpha\nu} = \Delta N^F_{\alpha\nu,+1} - \Delta N^F_{\alpha\nu,-1}$.

For excited energy eigenstates generated by processes involving pseudofermion occupancies in the vicinity of the $c0$ or $s1$ *Fermi points*, the functional (7) and the corresponding branch-line exponent expressions involve the following *Fermi*-point two-pseudofermion phase-shift parameters:

$$\xi^j_{\alpha\nu\alpha'\nu'} = \delta_{\alpha,\alpha'}\delta_{\nu,\nu'} + \sum_{\iota=\pm1}(\iota^j)\Phi_{\alpha\nu,\alpha'\nu'}(q^0_{F\alpha\nu}, \iota q^0_{F\alpha'\nu'}); \qquad j = 0, 1, \tag{8}$$

where $\alpha\nu = c0, s1$ and $\alpha'\nu' = c0, s1$. In the limit $m \to 0$, these parameters are given by $\xi^0_{c0c0} = 1/\xi_0$, $\xi^0_{c0s1} = 0$, $\xi^0_{s1c0} = -1/\sqrt{2}$, $\xi^0_{s1s1} = \sqrt{2}$, $\xi^1_{c0c0} = \xi_0$, $\xi^1_{c0s1} = \xi_0/2$, $\xi^1_{s1c0} = 0$ and $\xi^1_{s1s1} = 1/\sqrt{2}$. Here ξ_0 is the usual TTL parameter such that $\xi_0 \to \sqrt{2}$ and $\xi_0 \to 1$ as $U/t \to 0$ and $U/t \to \infty$, respectively.

We emphasize that the limits $m \to 0$, $U/t \to 0$ and $U/t \to 0$, $m \to 0$ do not commute and lead to different values for the parameters (8): while for $m \to 0$, $U/t \to 0$ one finds $\xi^0_{c0c0} \to 1/\sqrt{2}$, $\xi^0_{c0s1} \to 0$, $\xi^0_{s1c0} \to -1/\sqrt{2}$, $\xi^0_{s1s1} \to \sqrt{2}$, $\xi^1_{c0c0} \to \sqrt{2}$, $\xi^1_{c0s1} \to 1/\sqrt{2}$, $\xi^1_{s1c0} \to 0$ and $\xi^1_{s1s1} \to 1/\sqrt{2}$, for $U/t \to 0$, $m \to 0$ the result is $\xi^j_{c0c0} \to 1$, $\xi^j_{c0s1} \to 0$, $\xi^j_{s1c0} \to 0$ and $\xi^j_{s1s1} \to 1$ for both $j = 0$ and $j = 1$. Also the phase shifts $\Phi_{s1,c0}(k_{F\downarrow}, q)$ and $\Phi_{s1,s1}(k_{F\downarrow}, q)$ have different values in the limits $m \to 0$, $U/t \to 0$ and $U/t \to 0$, $m \to 0$, respectively. Therefore, for some excitations the spin functionals $2\Delta^{-1}_{s1}$ and $2\Delta^{+1}_{s1}$ have different values in these two limits. For such excitations we provide below the spectral-function exponent associated with the limit $U/t \to 0$, $m \to 0$, which is that which leads to the correct $U/t = 0$ spectral-function behaviour for $m = 0$. This can be confirmed by studying the limit of the corresponding exponents as $U/t \to 0$ for $m > 0$.

3.2. General expressions in the vicinity of the pseudofermion branch lines

Here and in section 4 we label the $\alpha\nu$ pseudofermions by their bare-momentum q. The momentum values k of the one-electron-removal $\alpha\nu$ branch-line points $(k, l\omega_{\alpha\nu}(k))$ are determined through the bare-momentum value q of the created $\alpha\nu$ pseudofermion or hole by the following parametric equations:

$$\begin{aligned} &k = -[k_0 - q]; \qquad q = [k + k_0]; \qquad \omega_{\alpha\nu} = -\epsilon_{\alpha\nu}(q); \\ &k_0 = 4k_F\Delta J^F_{c0} + 2k_{F\downarrow}\Delta J^F_{s1}. \end{aligned} \tag{9}$$

The one-electron-removal spectral function (2) has in the vicinity of the $\alpha\nu$ branch lines the following power-law expression for *finite* values of the energy $\omega < 0$ such that $-(\omega + \omega_{\alpha\nu}(q))$ is small and positive and $\omega_{\alpha\nu}(q) \neq 0$ where the point $(k, -\omega_{\alpha\nu}(q))$ belongs to the branch line [26]:

$$\begin{aligned} B(k,\omega) &\approx C_{\alpha\nu}(q)\Big(\frac{-[\omega + \omega_{\alpha\nu}(q)]}{4\pi\sqrt{v_{c0}v_{s1}}}\Big)^{\zeta_{\alpha\nu}(q)}; \qquad \zeta_{\alpha\nu}(q) > -1 \\ &= \delta\Big(\omega + \omega_{\alpha\nu}(q)\Big); \qquad \zeta_{\alpha\nu}(q) = -1; \quad \alpha\nu = c0, s1. \end{aligned} \tag{10}$$

Here the first expression is the leading-order term of a power-law expansion in the small energy deviation $-[\omega + \omega_{\alpha\nu}(k)]$ relative to the branch-line energy whose exponent $\zeta_{\alpha\nu}(k)$ and

pre-factor $C_{\alpha\nu}(k)$ have the following general form:

$$\zeta_{\alpha\nu}(q) = -1 + \zeta_0(q);$$
$$\zeta_0(q) = 2\Delta_{c0}^{+1}(q) + 2\Delta_{c0}^{-1}(q) + 2\Delta_{s1}^{+1}(q) + 2\Delta_{s1}^{-1}(q) \geqslant 0;$$
$$C_{\alpha\nu}(q) = \frac{\mathrm{sgn}\,(q)1}{2\pi}\int_{-\frac{\mathrm{sgn}\,(q)1}{v_{s1}}}^{\frac{I_{\alpha\nu}(q)}{v_{\alpha\nu}(q)}} \mathrm{d}z \frac{F_0(z)}{[1 - z v_{\alpha\nu}(q)]^{\zeta_0(q)}} \geqslant 0; \qquad v_{s1} \leqslant \frac{|v_{\alpha\nu}(q)|}{I_{\alpha\nu}(q)} \tag{11}$$
$$= \frac{\mathrm{sgn}\,(q)1}{2\pi}\int_{-\frac{\mathrm{sgn}\,(q)1}{v_{s1}}}^{\frac{\mathrm{sgn}\,(q)1}{v_{s1}}} \mathrm{d}z \frac{F_0(z)}{[1 - z v_{\alpha\nu}(q)]^{\zeta_0(q)}} \geqslant 0; \qquad v_{s1} \geqslant \frac{|v_{\alpha\nu}(q)|}{I_{\alpha\nu}(q)}.$$

In these expressions $I_{\alpha\nu}(q) = [1 + [\omega + \omega_{\alpha\nu}(q)]/\Omega]$ and the small positive energy Ω corresponds to the energy range of the small-momentum and low-energy $c0$ and $s1$ pseudofermion particle–hole elementary processes. In the numerical evaluation of the spectral-function expressions the value of Ω is determined by the normalization procedure associated with imposing the k and ω spectral-function sum rules [26]. Moreover, in the above equations $F_0(z)$ is an even function of z which for the branch-line excitations considered in this paper can have two alternative expressions. If the two charge parameters $2\Delta_{c0}^{\pm}(q)$ and two spin parameters $2\Delta_{s1}^{\pm 1}(q)$ given in equation (7) have finite values it is given by

$$F_0(z) = 2D_0\sqrt{\frac{v_{s1}}{v_{c0}}}\int_0^1 \mathrm{d}x \int_{-1}^{+1}\mathrm{d}y \prod_{\iota'=\pm 1}\frac{\Theta\left(1 - x + \mathrm{sgn}\,(z)\iota'\left[v_{s1}|z| - \frac{v_{s1}}{v_{c0}}y\right]\right)}{\Gamma(2\Delta_{s1}^{\iota'})}$$
$$\times \frac{\Theta\left(x + \mathrm{sgn}\,(z)\iota' y\right)}{\Gamma(2\Delta_{c0}^{\iota'})}\left(\sqrt{\frac{v_{c0}}{v_{s1}}}\left[1 - x + \mathrm{sgn}\,(z)\iota'\left[v_{s1}|z| - \frac{v_{s1}}{v_{c0}}y\right]\right]\right)^{2\Delta_{s1}^{\iota}-1}$$
$$\times \left(\sqrt{\frac{v_{s1}}{v_{c0}}}\left[x + \mathrm{sgn}\,(z)\iota' y\right]\right)^{2\Delta_{c0}^{\iota'}-1}, \tag{12}$$

where

$$D_0 = [N_a]^{-2+\zeta_0(q)}\prod_{\alpha\nu=c0,s1} A_{\alpha\nu}^{(0,0)}, \tag{13}$$

and $A_{\alpha\nu}^{(0,0)}$ is the $\alpha\nu$ pseudofermion lowest-peak weight functional

$$A_{\alpha\nu}^{(0,0)} = \left(\frac{1}{N_{\alpha\nu}^*}\right)^{2[N_{\alpha\nu}^0 + \Delta N_{\alpha\nu}]}\prod_{q_j\in\mathcal{F}}\sin^2\frac{Q_{\alpha\nu}(q_j)}{2}\prod_{j=1}^{N_{\alpha\nu}^*-1}\left(\sin\frac{\pi j}{N_{\alpha\nu}^*}\right)^{2(N_{\alpha\nu}^*-j)}$$
$$\times \prod_{q_i\in\mathcal{F}}\prod_{q_j\in\mathcal{F}}\theta(q_j - q_i)\sin^2\frac{Q_{\alpha\nu}(q_j)/2 - Q_{\alpha\nu}(q_i)/2 + \pi(j-i)}{N_{\alpha\nu}^*}$$
$$\times \prod_{q_i\in\mathcal{F}}\prod_{q_j\in\mathcal{F}}\sin^{-2}\frac{\pi(j-i) + Q_{\alpha\nu}(q_j)/2}{N_{\alpha\nu}^*}; \qquad \alpha\nu = c0, s1. \tag{14}$$

Here $\theta(x) = 1$ for $x > 0$, $\theta(x) = 0$ for $x \leqslant 0$, $N_{\alpha\nu}^*$ is the number of $\alpha\nu$-band discrete bare-momentum values q_j, $j = 1, 2, \ldots, N_{\alpha\nu}^*$ of the excited states such that $N_{c0}^* = N_a$ and $N_{s1}^* = N_{c0}^0 - N_{s1}^0 + \Delta N_{c0} - \Delta N_{s1}$, $Q_{\alpha\nu}(q_j)/2$ is the overall phase shift $Q_{\alpha\nu}(q)/2 = Q_{\alpha\nu}^0/2 + Q_{\alpha\nu}^{\Phi}(q)/2$ associated with the overall scattering phase shift $Q_{\alpha\nu}^{\Phi}(q)/2$, equation (3), and $q_j \in \mathcal{F}$ corresponds to the set of discrete bare-momentum values in the range $q_{\mathrm{F}\alpha\nu,-1} \leqslant q_j \leqslant q_{\mathrm{F}\alpha\nu,+1}$ where $q_{\mathrm{F}\alpha\nu,\iota} = \iota q_{\mathrm{F}\alpha\nu}^0 + \Delta q_{\mathrm{F}\alpha\nu,\iota}$ and $\Delta q_{\mathrm{F}\alpha\nu,\iota} = \iota[2\pi/L]\Delta N_{\alpha\nu,\iota}^{\mathrm{F}}$.

The weight D_0, equation (13), is independent of N_a. Indeed, a suitable handling of expression (14) reveals that the factor $[N_a]^{-2+\zeta_0(q)}$ exactly cancels the N_a dependence of $A_{\alpha\nu}^{(0,0)}$. Expression (12) is that provided for $F_0(z)$ in [26]. It is valid for the density ranges $0 < n < 1$

and $0 < m < n$ such that the above four parameters are always finite. However, for the $m \to 0$ limit considered in this paper it occurs for some excitations that one of the two spin parameters $2\Delta_{s1}^{\pm 1}(q)$ vanishes. If one considers that $2\Delta_{s1}^{-\iota} = 0$ and the remaining three parameters are finite the function $F_0(z)$ reads instead

$$F_0(z) = 2D_0\frac{v_{s1}}{v_{c0}}\int_{-1}^{+1}\mathrm{d}y\frac{\Theta\Big(\iota\Big[\mathrm{sgn}\,(z)y - v_{c0}\big(z - \frac{\iota}{v_{s1}}\big)\Big]\Big)\Theta\Big(\iota[zv_{c0} - \mathrm{sgn}\,(z)y]\Big)}{\Gamma(2\Delta_{s1}^{\iota})}$$
$$\times\left(\sqrt{\frac{v_{c0}}{v_{s1}}}2\iota\Big[z - \mathrm{sgn}\,(z)\frac{y}{v_{c0}}\Big]v_{\tilde{\alpha}\tilde{\nu}}\right)^{2\Delta_{\tilde{\alpha}\tilde{\nu}}^{\tilde{\iota}}-1}$$
$$\times\prod_{\iota'=\pm 1}\frac{\Theta\Big(1 + \mathrm{sgn}\,(z)\big[\iota' + \iota\frac{v_{s1}}{v_{c0}}\big]y - \iota v_{s1}z\Big)}{\Gamma(2\Delta_{c0}^{\iota'})}$$
$$\times\left(\sqrt{\frac{v_{s1}}{v_{c0}}}\Big[1 + \mathrm{sgn}\,(z)\Big[\iota' + \iota\frac{v_{s1}}{v_{c0}}\Big]y - \iota v_{s1}z\Big]\right)^{2\Delta_{c0}^{\iota'}-1}. \qquad (15)$$

A full quantitative study of the pre-factor $C_{\alpha\nu}(q)$ whose general expression is defined by equations (11)–(15) involves the numerical derivation of the lowest-peak weight $A_{\alpha\nu}^{(0,0)}$, equation (14), for each excited energy eigenstate contributing to the one-electron spectral weight. Such a quantitative study, which requires involved numerical calculations, is beyond the goals of this paper and will be carried out elsewhere. However, the general $C_{\alpha\nu}(q)$ expression defined above is useful for our studies, once it can be used to extract information about the behaviour of the pre-factor $C_{\alpha\nu}(q)$ as $U/t \to 0$ and find out whether for finite values of U/t that function is vanishing or finite and also what its relative value for different branch lines is.

A $\alpha\nu$ branch line whose exponent $\zeta_{\alpha\nu}(q)$ is negative for a given domain of $k = -[k_0 - q]$ values is called a singular branch line. In this case the weight distribution shows a singular behaviour at the branch line, and we expect that the spectral peaks will be observed in a real experiment. This was confirmed for the present case of one-electron removal, as discussed in section 5. On the other hand, when for a (k, ω)-plane region in the vicinity of the branch line and contained inside the one-electron-removal dominant-weight domain of figure 1 of [30] the exponent (11) is such that $0 < \zeta_{\alpha\nu}(q) < 1$, the spectral feature refers to an edge branch line. Finally, $0 < \zeta_{\alpha\nu}(q) < 1$ for regions away from that domain and $\zeta_{\alpha\nu}(q) > 1$ for any (k, ω)-plane region are in general a sign of a near absence of spectral weight. For one-electron removal, and thus $\omega < 0$, the singular and edge branch lines are represented in figure 1 of [30] by solid and dashed lines, respectively. The dashed–dotted lines of that figure are either limiting lines for the domain of weight generated by dominant processes or lines associated with exponents larger than one. The lowest limiting line of the figure corresponds to a singular but weak spectral feature called a border line, as mentioned in section 5.

The general branch-line spectral-function expressions defined by equations (10) and (11) are not valid in the vicinity of the low-energy branch-line end points. These end points correspond to values of k and ω such that $\omega \approx \iota v_{\alpha\nu}(k + k_0^{\mathrm{F}})$ where,

$$k_0^{\mathrm{F}} = k_0 - \iota q_{\mathrm{F}\alpha\nu}^0; \qquad \alpha\nu = c0, s1, \quad \iota = \pm 1,$$

and k_0 is the momentum given in equation (9). In this low-energy limit the physics is that of the so-called low-energy TLL regime, where bosonization [10] and conformal-field theory [11–19] are applicable.

3.3. Limiting low-energy behaviour near the branch-line end points

The $\alpha\nu = c0, s1$ branch lines also exist for *small* positive values of $-\omega$. Such a regimen corresponds to the above-mentioned values of k and ω such that $\omega \approx \iota v_{\alpha\nu}(k + k_0^{\mathrm{F}})$. In this case the expression (10) does not apply and instead the general PDT leads to the following one-electron-removal spectral-function expression [26]:

$$B(k,\omega) \propto \left(\frac{-[\omega + \iota v_{\alpha\nu}(k + k_0^{\mathrm{F}})]}{4\pi\sqrt{v_{c0}v_{s1}}}\right)^{-1+\zeta^0_{\alpha\nu,\iota}}; \qquad \zeta^0_{\alpha\nu,\iota} = \zeta^0_{\alpha\nu} - 2\Delta^{-\iota}_{\alpha\nu} \geqslant 0, \tag{16}$$

where $\alpha\nu = c0, s1$, $\iota = \pm 1$. The low-energy spectral function expression given in equation (16) refers in general to the proximity of a $\alpha\nu = c0, s1$ branch-line end point. In turn, the finite-energy expression (10) applies in the vicinity of the $\alpha\nu = c0, s1$ branch lines when the $\alpha\nu = c0, s1$ branch-line group velocity $v_{\alpha\nu}(q)$ is such that $v_{\alpha\nu}(q) \neq \iota v_{\alpha\nu}$. As the value of $v_{\alpha\nu}(q)$ approaches that of the *Fermi point* velocities $\pm v_{\alpha\nu}$, $v_{\alpha\nu}(q) \to \iota v_{\alpha\nu}$, the spectral function k and ω values reach the vicinity of a branch-line end point and thus the spectral function is given by expression (16) instead of (10).

Interestingly, for $\omega \approx \iota v_{\alpha\nu}(k - lk_0^{\mathrm{F}})$ in the momentum expression (9), the validity of the spectral-function expression given in equation (16) corresponds to the TLL regime. Therefore, in this limit the above exponent $-1 + \zeta^0_{\alpha\nu,\iota}$ provided by the general PDT of [26] must equal that corresponding to the low-energy universal TLL expressions. Indeed, it is straightforward to show that the general exponent $-1 + \zeta^0_{\alpha\nu,\iota}$ of expression (16) is identical to that given in equation (5.7) of [16]. When applied to specific spectral functions such that $\omega < 0$, expression (16) provides the universal and well known low-energy TLL behaviour for the 1D Hubbard model [11–19], the Tomonaga–Luttinger model [34–36] and many other models whose low-energy physics corresponds to the same universality class. When $-1 + \zeta^0_{\alpha\nu,\iota} < 0$, such an expression refers to a linear singular spectral feature.

There is a cross-over region between the finite-energy and low-energy regimens corresponding to the spectral-function expressions (10) and (16), respectively. The momentum and energy width corresponding to such a crossover regimen is very small and is fully controlled by the value of $|v_{\alpha\nu}(q) - \iota v_{\alpha\nu}|$. The low-energy TLL behaviour emerges when $|v_{\alpha\nu}(q) - \iota v_{\alpha\nu}| \approx |a_{\alpha\nu}(q^0_{\mathrm{F}\alpha\nu})(k + k_0^{\mathrm{F}})|$, where $a_{\alpha\nu}(q) = \partial v_{\alpha\nu}(q)/\partial q$ for $\alpha\nu = c0, s1$. As the value of the branch-line bare-momentum q of equation (9) approaches $\iota q^0_{\mathrm{F}\alpha\nu}$ the behaviour (16) is reached. Importantly, for smaller values of $|a_{\alpha\nu}(q^0_{\mathrm{F}\alpha\nu})|$ the value of $|v_{\alpha\nu}(q) - \iota v_{\alpha\nu}|$ can remain small for larger values of $|k + k_0^{\mathrm{F}}|$ and thus of $\omega \approx \iota v_{\alpha\nu}(k + k_0^{\mathrm{F}})$. It follows that the momentum and energy widths of the (k, ω)-plane region in the vicinity of the point $(-k_0^{\mathrm{F}}, 0)$ where the TLL liquid behaviour is valid increase for decreasing values of $|a_{\alpha\nu}(q^0_{\mathrm{F}\alpha\nu})|$, provided that $v_{\alpha\nu}$ is finite. For instance, in the limit of zero spin density, $m \to 0$, the value of $|a_{s1}(q)|$ is small in two relatively large q regions in the vicinity of $q = -k_{\mathrm{F}}$ and $q = +k_{\mathrm{F}}$, respectively, and thus the domain of the corresponding spin $s1$ branch lines where the TLL expression (16) is valid increases in that limit. (We recall that the general exponent (11) cannot be obtained by the TLL low-energy methods.)

When the above branch-line end point $(-k_0^{\mathrm{F}}, 0)$ is reached through low-energy lines other than the above branch lines the spectral-function expression is different from (16). Examples of such points are the points $(k = k_{\mathrm{F}}, \omega = 0)$ and $(k = 3k_{\mathrm{F}}, \omega = 0)$ shown in figure 1 of [30]. The general theory provides spectral-function expressions that are valid when these points are approached by lines that are contained in the finite-weight regions and do not cross the $\alpha\nu$ branch lines ending at the same points. The velocity $v = 1/z = (\omega/(k + k_0^{\mathrm{F}})$ plays an important role in these expressions. Indeed, following the studies of [26], in the proximity of the point $(-k_0^{\mathrm{F}}, 0)$ but for values of k and ω such that $\omega \approx v(k + k_0^{\mathrm{F}})$, where $v \neq \pm v_{s1}, \pm v_{c0}$ and depending on the specific point, the $z = 1/v$ domain is bounded by two of the four values

$-1/v_{c0}$, $-1/v_{s1}$, $1/v_{s1}$, and $1/v_{c0}$, the momentum and energy weight-distribution dependence has the following general expression for finite values of U/t:

$$B(k,\omega) \approx \frac{F_0(1/v)}{4\pi\sqrt{v_{c0}v_{s1}}}\Big(\frac{-\omega}{4\pi\sqrt{v_{c0}v_{s1}}}\Big)^{-2+\zeta_0}; \qquad -2+\zeta_0 > -1, \tag{17}$$

where $F_0(z)$ is the function defined in equations (12) and (15) and ζ_0 is the above functional $\zeta_0 = 2\Delta_{c0}^{+1} + 2\Delta_{c0}^{-1} + 2\Delta_{s1}^{+1} + 2\Delta_{s1}^{-1}$. Here $2\Delta_{\alpha\nu}^{\iota}$ is the functional of equation (7) for the deviations of the bare-momentum distribution function associated with the excitations that control the spectral-weight distribution in the vicinity of the point $(-k_0^{\rm F}, 0)$.

Since the power-law spectral-function expressions (16) and (17) refer to the vicinity of low-energy lines and isolated zero-energy points in the (k,ω)-plane, respectively, that are not of interest for the low-energy phase of the organic compound TTF-TCNQ, here we limit our study to the more complex problem of the finite-energy branch-line spectral weight. Indeed, the low-energy phase of TTF-TCNQ is not metallic and refers to broken-symmetry states [1, 2], whereas the branch-line spectral features given by equation (10) refer to finite-energy values which correspond to the unusual metallic state of that organic compound.

4. The one-electron-removal branch lines

In this section we use the general branch-line expressions and associated quantities considered above in the study of the one-electron-removal finite-energy spectral-function singular and edge branch lines. The ground-state–excited-energy-eigenstate transitions to the subspace whose pseudofermion number deviations are given in equation (5), generate several $\alpha\nu$ pseudofermion branch lines whose location in the (k,ω)-plane is shown in figure 1 of [30] for $\omega < 0$. The $s \equiv s1$ branch line shown in the figure, which connects the points $(k = -k_{\rm F}, \omega = 0)$ and $(k = k_{\rm F}, \omega = 0)$, is generated by creating the $c0$ pseudofermion hole at one of its *Fermi* points, and the $s1$ pseudofermion hole for bare-momentum values in the domain defined by the inequality $|q| \leqslant k_{\rm F}$. We emphasize that in addition to creation of a $c0$ pseudofermion hole at $q = 2k_{\rm F}$ (and $q = -2k_{\rm F}$), this excitation includes a collective bare-momentum shift $Q_{c0}^0/L = +\pi/L$ (and $Q_{c0}^0/L = -\pi/L$) for the whole $c0$ pseudofermion *Fermi sea*.

By considering the same processes, plus transferring a $c0$ pseudofermion from the *Fermi point* $-\iota' 2k_{\rm F}$ to the *Fermi point* $\iota' 2k_{\rm F}$, two other $s1$ branch lines are generated, which connect the points $(k = -\iota' 3k_{\rm F}, \omega = 0)$ and $(k = -\iota' 5k_{\rm F}, \omega = 0)$ where $\iota' = \pm 1$. The $\iota' = -1$ line is labelled by s in figure 1 of [30], where it appears for $\omega \leqslant 0$. On the other hand, there are four $c0$ pseudofermion branches lines which connect the points $(k = -3k_{\rm F}, \omega = 0)$ and $(k = k_{\rm F}, \omega = 0)$, $(k = -k_{\rm F}, \omega = 0)$ and $(k = 3k_{\rm F}, \omega = 0)$, $(k = -5k_{\rm F}, \omega = 0)$ and $(k = -k_{\rm F}, \omega = 0)$ and $(k = k_{\rm F}, \omega = 0)$ and $(k = 5k_{\rm F}, \omega = 0)$. The first, second and fourth of these lines are labelled by c, c' and c'', respectively, in figure 1 of [30], where their $k > 0$ parts are shown for $\omega \leqslant 0$. Below we study the spectral-weight distribution in the vicinity of these seven one-electron-removal branch lines.

We start by evaluating the weight distribution corresponding to the first $s1$ pseudofermion branch line mentioned above. The specific form of the general expressions (9) for the points $(k, -\omega_{s1}(k))$ belonging to the $s1$ pseudofermion branch line in the $m \to 0$ limit corresponds to $k_0 = 0$ and reads

$$q = k; \qquad -\omega_{s1}(q) = \epsilon_{s1}(q). \tag{18}$$

Here $\epsilon_{s1}(q)$ is the energy dispersion given in equation (C.16) of [24] and plotted for $m \to 0$ in figure 7 of [25]. (The energy dispersions $\epsilon_{c0}(q)$ and $\epsilon_{s1}(q)$ appearing in other expressions of this section are those defined in equations (C.15) and (C.16) of [24] and plotted in figures 6 and

7 of [25], respectively.) We recall that the $k > 0$ part of this $s1$ pseudofermion singular branch line is labelled by s in figure 1 of [30], where it connects the points $(k = 0, \omega = \epsilon_{s1}(0))$ and $(k = k_{\rm F}, \omega = 0)$. In this case the general spectral-function expression (10) applies provided that the specific expression associated with the excitations around the point $(k, -\omega_{s1}(k))$ of the functional $2\Delta^{\iota}_{\alpha\nu}$ defined in equation (7) is used. This expression is a function of $k = q$ and corresponds to the $m \rightarrow 0$ limit of the following quantity:

$$2\Delta^{\iota}_{\alpha\nu}(q) = \left\{-\iota\frac{\xi^0_{\alpha\nu c0}}{2} - \Phi_{\alpha\nu,s1}(\iota q^0_{{\rm F}\alpha\nu}, q)\right\}^2; \qquad \alpha\nu = c0, s1. \tag{19}$$

Here the value of the two-pseudofermion phase shift $\Phi_{\alpha\nu,s1}$ and that of the two-pseudofermion phase shifts $\Phi_{\alpha\nu,\alpha'\nu'}$ appearing in other expressions of this section is uniquely defined in terms of the solution of a system of integral equations [26] and the general expression for the parameter $\xi^0_{\alpha\nu c0}$ is provided in equation (8).

Direct use of expression (10) in the $m \rightarrow 0$ limit, leads to the following expression for the one-electron removal spectral function:

$$\begin{aligned} B(k,\omega) &\approx C_{s1}(q)\left(\frac{-[\omega + \omega_{s1}(q)]}{4\pi\sqrt{v_{c0}v_{s1}}}\right)^{\zeta_{s1}(q)}; \qquad \zeta_{s1}(q) > -1 \\ &= \delta\big(\omega + \omega_{s1}(q)\big); \qquad \zeta_{s1}(q) = -1, \end{aligned} \tag{20}$$

which corresponds to energy values just below the branch line for $\zeta_{s1}(q) > -1$ and at that line for $\zeta_{s1}(q) = -1$ and to bare-momentum and momentum values in the range $-k_{\rm F} < q < k_{\rm F}$ and $-k_{\rm F} < k < k_{\rm F}$, respectively. The pre-factor $C_{s1}(q)$ given in equation (11) is finite for all values of the q domain, except in the vicinity of the branch-line end points, where $v_{s1}(q) \approx \pm v_{s1}$ and provided that $\zeta_{s1}(q) > -1$ the spectral function is instead of the form given in equation (16). When $\zeta_{s1}(q) = -1$ the second spectral-function expression of equation (20) applies. It refers to the whole branch-line momentum domain.

As the spin density m approaches zero, we find the following exponent expression valid for all values of U/t and electronic density n:

$$\begin{aligned} \zeta_{s1}(q) &= -1 + \sum_{\alpha\nu=c0,s1}\sum_{\iota=\pm1}\left\{\frac{\xi^0_{\alpha\nu c0}}{2} + \iota\Phi_{\alpha\nu,s1}(\iota q^0_{{\rm F}\alpha\nu}, q)\right\}^2 \\ &= 1 + \sum_{\iota=\pm1}\left\{\frac{1}{2\xi_0} + \iota\Phi_{c0,s1}(\iota 2k_{\rm F}, q)\right\}^2 + \sum_{\iota=\pm1}\left\{-\frac{1}{2\sqrt{2}} + \iota\Phi_{s1,s1}(\iota k_{\rm F}, q)\right\}^2, \end{aligned} \tag{21}$$

where the second expression was obtained by taking the limit $m \rightarrow 0$ in the first-expression quantities and ξ_0 is the usual TTF parameter. The dependence of the exponent (21) on the momentum k is obtained by combining equations (18) and (21). The exponent ζ_{s1} of equation (21) is negative for all values of momentum and is plotted in figure 1 as a function of the momentum k for $k > 0$, several values of U/t and electronic density $n = 0.59$. So the corresponding spectral-function expression (20) describes a singular branch line. The exponent ζ_s of the figure is the exponent (21) for momentum values $0 < k < k_{\rm F}$, whereas for $k_{\rm F} < k < 3k_{\rm F}$ ζ_s it corresponds to a one-electron addition exponent considered in [30].

While for momentum values $0 < k < k_{\rm F}$ one reaches the same value for the exponent plotted in figure 1 in the limits $m \rightarrow 0$, $U/t \rightarrow 0$ and $U/t \rightarrow 0$, $m \rightarrow 0$, that value is different for $k_{\rm F} < k < 3k_{\rm F}$. In this paper we always consider the limit $U/t \rightarrow 0$, $m \rightarrow 0$, whereas the studies of [30] considered the limit $m \rightarrow 0$, $U/t \rightarrow 0$. This justifies the different values of that exponent for $k_{\rm F} < k < 3k_{\rm F}$ and $U = 0$ given in figure 1 and in figure 2 of [30], respectively, which otherwise correspond to the same exponent values. The $U/t \rightarrow 0$ and $U/t \rightarrow \infty$

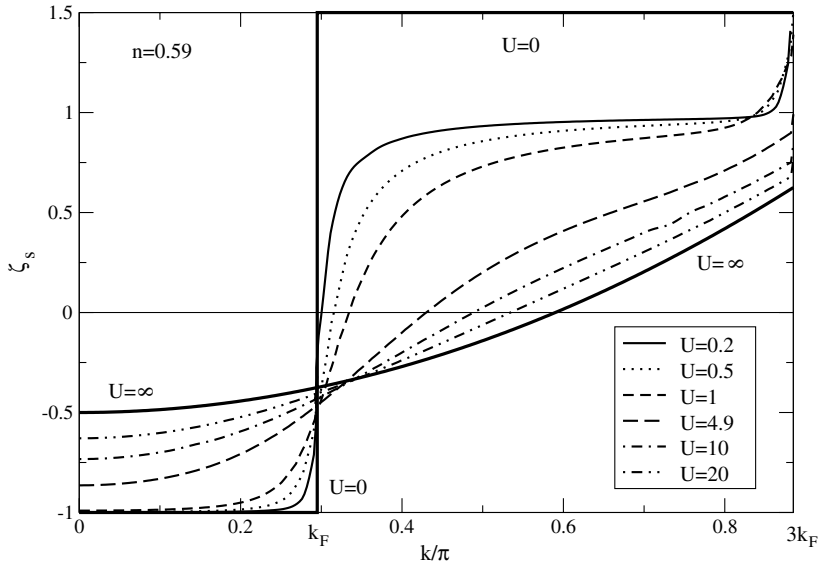

Figure 1. Momentum dependence of the exponents associated with the one-electron-removal spin $s \equiv s1$ branch line of figure 1 of [30] for $0 < k < k_F$ and one-electron addition spin branch line of the same figure for $k_F < k < 3k_F$. For the one-electron removal case considered here that exponent is given in equation (21). (In the figure both these exponents are called ζ_s.) We note that for $U > 0$ and in the one-electron-removal small-momentum domain in the vicinity of the branch-line end point $k = k_F$, where $v_{s1}(q) \approx v_{s1}$, the exponent plotted here does not apply, since the spectral function is instead of the form given in equation (16).

limiting values of the exponent (21) and other exponents obtained below are further discussed at the end of this section.

Similar results are obtained for the other two one-electron-removal $s1$ branch lines, whose exponent was not studied in [30]. We call them $s1, \iota'$ branch lines where $\iota' = \pm 1$. Here and in the expressions provided below we use the indices $\iota' = \pm 1$ and $\iota'' = \pm 1$ to denote contributions from processes which involve $c0$ and $s1$ pseudofermions, respectively, created or annihilated at the $m \rightarrow 0$ *Fermi points* $\iota' 2k_F = \pm 2k_F$ and $\iota'' k_F = \pm k_F$, respectively. For the $s1, \iota'$ branch lines, the index ι' refers to a $c0$ pseudofermion particle–hole process such that a $c0$ pseudofermion is annihilated at $q = -\iota' 2k_F$ and created at $q = \iota' 2k_F$, where $\iota' = \pm 1$. The specific form of the general expressions (9) for the points $(k, \omega_{s1,\iota'}(k))$ belonging to the $s1, \iota'$ branch line in the $m \rightarrow 0$ limit, corresponds to $k_0 = \iota' 4k_F$ and is given by

$$q = k + \iota' 4k_F; \qquad \omega_{s1,\iota'}(q) = -\epsilon_{s1}(q). \tag{22}$$

The $s1, -1$ pseudofermion singular branch line is labelled by s in figure 1 of [30], where for $\omega/t < 0$ it connects the points $(k = 3k_F, \omega = 0)$ and $(k = 5k_F, \omega = 0)$. In this case the value of the functional (7) is a function of $k = q + \iota' 4k_F$ given by the $m \rightarrow 0$ limit of the parameter

$$2\Delta^{\iota}_{\alpha\nu}(q) = \left\{ -\iota \frac{\xi^0_{\alpha\nu c0}}{2} + \iota' \xi^1_{\alpha\nu c0} - \Phi_{\alpha\nu,s1}(\iota q^0_{F\alpha\nu}, q) \right\}^2; \qquad \alpha\nu = c0, s1. \tag{23}$$

Use of the general expression (10) in the $m \rightarrow 0$ limit, leads to the following expression for the one-electron-removal spectral function:

$$B(k,\omega) \approx C_{s1,\iota'}(q)\left(\frac{-[\omega+\omega_{s1,\iota'}(q)]}{4\pi\sqrt{v_{c0}v_{s1}}}\right)^{\zeta_{s1,\iota'}(q)}. \tag{24}$$

This expression corresponds to energy values just below the branch line and to bare-momentum values in the range $-k_{\rm F} < q < k_{\rm F}$ and momentum values in the domains $-5k_{\rm F} < k < -3k_{\rm F}$ and $3k_{\rm F} < k < 5k_{\rm F}$ for $\iota' = 1$ and $\iota' = -1$, respectively. In the $m \rightarrow 0$ limit, we find the following exponent expression valid for all values of U/t and electronic density n:

$$\begin{aligned}\zeta_{s,\iota'}(q) &= -1 + \sum_{\alpha\nu=c0,s1}\sum_{\iota=\pm1}\left\{\frac{\xi^0_{\alpha\nu c0}}{2} - \iota'\xi^1_{\alpha\nu,c0} + \iota\Phi_{\alpha\nu,s1}(\iota q^0_{{\rm F}\alpha\nu}, q)\right\}^2 \\ &= 1 + \sum_{\iota=\pm1}\left\{\frac{1}{2\xi_0} - \iota'\xi_0 + \iota\Phi_{c0,s1}(\iota 2k_{\rm F}, q)\right\}^2 \\ &\quad + \sum_{\iota=\pm1}\left\{-\frac{1}{2\sqrt{2}} + \iota\Phi_{s1,s1}(\iota k_{\rm F}, q)\right\}^2. \end{aligned} \tag{25}$$

The dependence of the exponent (25) on the momentum k is obtained by combining equations (22) and (25). For most of the parameter space and bare-momentum values, this exponent is larger than one and thus the spectral-function expression (24) does not describe a branch line. Consistently, for finite values of U/t the pre-factor $C_{s1,\iota'}(q)$ of equation (24) has smaller values than those of the pre-factor $C_{s1}(q)$ appearing in expression (20). However, for large values of U/t and bare-momentum values in the vicinity of $\iota' k_{\rm F}$ such an exponent corresponds to a branch line, as it reaches values smaller than one. We recall that for small domains in the vicinity of the end points $k = \pm 3k_{\rm F}$ and $k = \pm 5k_{\rm F}$ the spectral function is not of the form (24), but instead is of the general form given in equation (16).

Equivalent results are obtained for the four $c0, \iota', \iota''$ branch lines, where $\iota', \iota'' = \pm 1$. In this case, the specific form of the general expressions (9) for the points $(k, \omega_{c0,\iota',\iota''}(k))$ belonging to the $c0, \iota', \iota''$ branch lines in the $m \rightarrow 0$ limit, corresponds to $k_0 = \iota' 2k_{\rm F} - \iota'' k_{\rm F}$ and reads

$$q = k + \iota' 2k_{\rm F} - \iota'' k_{\rm F}; \qquad \omega_{c0,\iota',\iota''}(q) = -\epsilon_{c0}(q). \tag{26}$$

The $c0, +1, +1$ branch line, the $c0, -1, -1$ branch line and the $c0, -1, +1$ branch line are labelled c, c' and c'' in figure 1 of [30], respectively, where they are represented for $k > 0$ and $\omega \leqslant 0$. In this case the value of the functional (7) is given by the $m \rightarrow 0$ limit of the following parameter:

$$2\Delta^{\iota}_{\alpha\nu}(q) = \left\{\iota'\frac{\xi^1_{\alpha\nu c0}}{2} - \iota\frac{\xi^0_{\alpha\nu s1}}{2} - \iota''\frac{\xi^1_{\alpha\nu s1}}{2} - \Phi_{\alpha\nu,c0}(\iota q^0_{{\rm F}\alpha\nu}, q)\right\}^2, \tag{27}$$

where $\alpha\nu = c0, s1$.

The dependence of this quantity on the momentum k is obtained by combining equations (26) and (27). From use of the general expression (10) in the $m \rightarrow 0$ limit, we find the following expression for the one-electron-removal spectral function:

$$B(k,\omega) \approx C_{c0,\iota',\iota''}(q)\left(\frac{-[\omega+\omega_{c0,\iota',\iota''}(q)]}{4\pi\sqrt{v_{c0}v_{s1}}}\right)^{\zeta_{c0,\iota',\iota''}(q)}. \tag{28}$$

This expression corresponds to energy values just below the branch lines. In this expression and in the exponent expressions provided below, the bare-momentum values are in the range $-2k_{\rm F} < q < 2k_{\rm F}$. Furthermore, the corresponding momentum values belong to the domains $-3k_{\rm F} < k < k_{\rm F}$ and $-k_{\rm F} < k < 3k_{\rm F}$ for $\iota' = \iota'' = 1$ and $\iota' = \iota'' = -1$, respectively, and $-5k_{\rm F} < k < -k_{\rm F}$ and $k_{\rm F} < k < 5k_{\rm F}$ for $\iota' = -\iota'' = 1$ and $\iota' = -\iota'' = -1$, respectively. In the

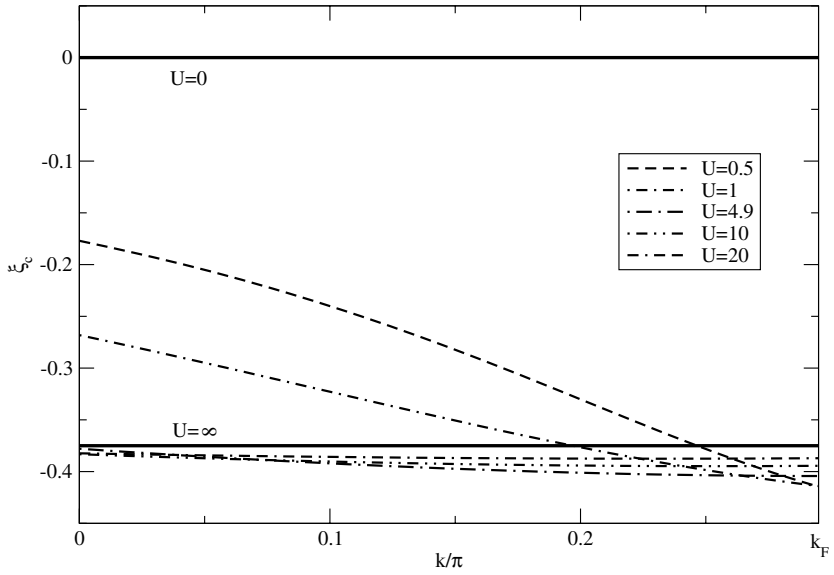

Figure 2. Momentum dependence of the exponent (29) along the one-electron-removal $c \equiv c0, +1, +1$ branch line of figure 1 of [30] for $0 < k < k_F$. In the figure that exponent is called ζ_c and is given by 0 and $-3/8$ for $U/t \rightarrow 0$ and $U/t \rightarrow \infty$, respectively. We note that for a small momentum domain in the vicinity of the branch-line end point $k = k_F$, where $v_{c0}(q) \approx v_{c0}$, this exponent does not apply, since the spectral function is of the form given in equation (16).

$m \rightarrow 0$ limit, the exponent $\zeta_{c0,\iota',\iota''}(q)$ of expression (28) reads

$$\begin{aligned}\zeta_{c0,\iota',\iota''}(q) &= -1 + \sum_{\alpha\nu=c0,s1}\sum_{\iota=\pm 1}\left\{-\iota\iota'\frac{\xi^1_{\alpha\nu c0}}{2} + \frac{\xi^0_{\alpha\nu s1}}{2} + \iota\iota''\frac{\xi^1_{\alpha\nu s1}}{2} + \iota\Phi_{\alpha\nu,c0}(\iota q^0_{F\alpha\nu}, q)\right\}^2 \\ &= 1 + \sum_{\iota=\pm 1}\left[\left\{-\iota\frac{\xi_0}{2}\left(\iota' - \frac{\iota''}{2}\right) + \iota\Phi_{c0,c0}(\iota 2k_F, q)\right\}^2\right. \\ &\quad \left. + \left\{\frac{1}{\sqrt{2}}\left(1 + \frac{\iota\iota''}{2}\right) + \iota\Phi_{s1,c0}(\iota k_F, q)\right\}^2\right]. \qquad (29)\end{aligned}$$

For $U/t > 0$ the exponent $\zeta_{c0,+1,+1}(q)$ of equation (29) is negative for all values of momentum, whereas $\zeta_{c0,-1,-1}(q)$ is also in general negative, except for small values of U/t and a small domain of bare-momentum values. These exponents are plotted in figures 2 and 3, respectively, as a function of the momentum k for $k > 0$, several values of U/t and electronic density $n = 0.59$. In these figures these exponents are called ζ_c and $\zeta_{c'}$, respectively. Correspondingly, when $\zeta_{c0,\iota',\iota''}(q) < 0$ the weight distribution (28) describes a singular branch line.

In turn, the exponents $\zeta_{c0,+1,-1}$ and $\zeta_{c0,-1,+1}$ of equation (29) are positive. For the values of momentum for which these exponents are smaller than one the spectral-function expression (28) describes edge branch lines. For finite values of U/t the pre-factors $C_{c0,\pm 1,\mp 1}(q)$ have in general smaller values than the pre-factors $C_{c0,\pm 1,\pm 1}(q)$. Moreover, for finite values of U/t the pre-factors $C_{c0,+1,+1}(q)$ and $C_{c0,-1,-1}(q)$ are decreasing and increasing functions of k, respectively, whose values are smallest for the domains $-3k_F < k < -2k_F$ and $2k_F < k < 3k_F$, respectively. Again, in the vicinity of the branch-line end points $k = \pm k_F$, $k = \pm 3k_F$, and $k = \pm 5k_F$, where $v_{c0}(q) \approx \pm v_{c0}$, the spectral function is not of the form (28), but instead is of the general form given in equation (16).

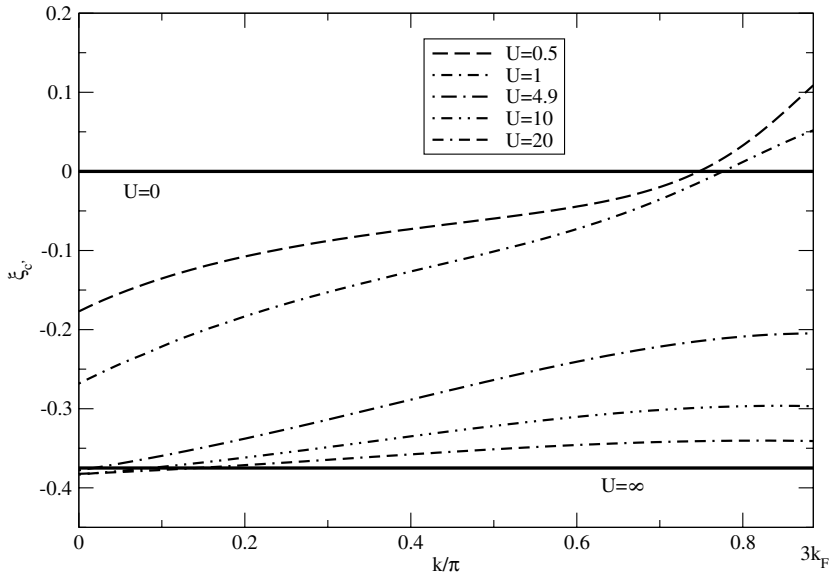

Figure 3. Momentum dependence of the exponent (29) along the one-electron-removal charge $c' \equiv c0, -1, -1$ branch line of figure 1 of [30] for $0 < k < 3k_F$. In the figure that exponent is called $\zeta_{c'}$ and is given by 0 and $-3/8$ for $U/t \rightarrow 0$ and $U/t \rightarrow \infty$, respectively. For a small momentum domain in the vicinity of the branch-line end point $k = 3k_F$, where $v_{c0}(q) \approx v_{c0}$, this exponent does not apply, since the spectral function is of the form given in equation (16).

The exponents plotted in figures 2 and 3 have different values in the limits $m \rightarrow 0$, $U/t \rightarrow 0$ and $U/t \rightarrow 0$, $m \rightarrow 0$. This justifies the different values of these exponents given for $U/t \rightarrow 0$ in figures 2 and 3 and in figure 3 of [30], respectively. However, there are differences for finite values of U/t as well. Indeed, by an error in the choice of the exponent expressions, the studies of that reference used an approximation such that one of the U/t-dependent functions contributing to the exponent expression (29) was replaced by its large-U/t asymptotic expansion. Therefore, for small and intermediate values of U/t the values provided here for that exponent are also different from those given in that reference. Our exact expression (29) and the corresponding figures 2 and 3 replace such an asymptotic expansion. The main correction to the preliminary results of [30] is that the exponent plotted in figure 3 becomes positive for small values of U/t and a small domain of momentum values in the vicinity of $3k_F$.

We finish this section by confirming that the momentum and energy dependence of the spectral-weight distribution in the vicinity of the corresponding branch lines in the limits $U/t \rightarrow 0$ and $U/t \rightarrow \infty$ recovers the correct behaviours. (We recall that in this paper we reach the limit $U/t \rightarrow 0$ by considering the limit $U/t \rightarrow 0$, $m \rightarrow 0$.) All expressions provided below are valid for electronic densities n such that $0 < n < 1$.

Independently of the general exponent expressions derived by the PDT of [26], we also used here the method of [20, 21] to derive the exponents associated with the one-electron-removal spectral function expressions obtained in these references for $U/t \rightarrow \infty$. The limiting values of the exponents obtained here fully agree with those obtained for $U/t \rightarrow \infty$ by use of the method of [20, 21]. Thus, our general U/t expressions are fully consistent with the spectral function expressions found in these references for $U/t \rightarrow \infty$.

Use of the general results of [26] for the one-electron-removal spectral function in the vicinity of the $s1$ branch line, which for finite values of U and energy ω is given by

expression (20), reveals that as $U/t \rightarrow 0$ the pre-factor $C_{s1}(q)$ corresponding to the general finite-energy expression (10) is replaced by the weight constant of the δ-peak spectral function given in the second expression of equation (10). The regimen associated with such a weight constant arises for very low values of U/t, where it is given by $(1/N_a)^{\zeta_0(q)} \rightarrow 1$ [26]. Its independence of the value of the bare-momentum q results from the behaviour of the functional $\zeta_0(q)$, which for this specific branch line is such that $\zeta_0(q) \rightarrow 0$ as $U/t \rightarrow 0$ for the whole corresponding domain of q values. We find that in the limits $U/t \rightarrow 0$ and $U/t \rightarrow \infty$, the $s1$ branch-line exponent given in equation (21) reads

$$\zeta_{s1}(q) = -1, \qquad U/t \rightarrow 0; \qquad \zeta_{s1}(q) = -\frac{1}{2} + 2\left(\frac{q}{4k_{\rm F}}\right)^2, \qquad U/t \rightarrow \infty, \tag{30}$$

for the q and k values of the spectral-function expression (20). In turn, the pre-factor of the low-energy power-law expression (16) vanishes as $U/t \rightarrow 0$. Thus, in that limit the second expression of equation (10) is valid for the whole branch-line bare-momentum domain and the regimen associated with the spectral-function expression (16) disappears. Moreover, according to equation (A2) of [25], in the limit $U/t \rightarrow 0$ the dispersion $\epsilon_{s1}(q)$ becomes the electronic spectrum $\epsilon_{s1}(q) = -2t[\cos(q) - \cos(k_{\rm F})]$. Consistently, according to equation (30), the exponent (21) is such that $\zeta_{s1}(q) \rightarrow -1$ as $U/t \rightarrow 0$ for all values of q in the range $0 < |q| < k_{\rm F}$ and thus of the momentum k in the domain $0 < |k| < k_{\rm F}$. Then, following the second expression of equation (20), the correct non-interacting one-electron-removal spectral function is reached in this limit.

For the one-electron-removal $s1, \iota'$ branch-line expression (24), the multiplicative coefficient is such that $C_{s1,\iota'}(q) \rightarrow 0$ as $U/t \rightarrow 0$. Thus, such a branch line does not exist for $U/t \rightarrow 0$, which is the correct result. For $m \rightarrow 0$ and in the limits $U/t \rightarrow 0$ and $U/t \rightarrow \infty$ the corresponding exponent (25) reads

$$\begin{aligned} &\zeta_{s1,\iota'}(q) = 3, \qquad U/t \rightarrow 0; \\ &\zeta_{s1,\iota'}(q) = \frac{3}{2} - \iota'\frac{q}{k_{\rm F}} + 2\left(\frac{q}{4k_{\rm F}}\right)^2, \qquad U/t \rightarrow \infty, \end{aligned} \tag{31}$$

for the q and k values of the spectral-function expression (24). In the limit $U/t \rightarrow \infty$, this exponent is such that $\zeta_{s1,\iota'}(q) = 5/8$ for $q \rightarrow \iota' k_{\rm F}$, $\zeta_{s1,\iota'}(q) = 3/2$ for $q = 0$, and $\zeta_{s1,\iota'}(q) = 21/8$ for $q \rightarrow -\iota' k_{\rm F}$. For the one-electron-removal $c0, \iota', \iota''$ branch-line expression (28), the multiplicative coefficient is such that $C_{c0,\iota',\iota''}(q) \rightarrow 0$ as $U/t \rightarrow 0$, which again is the correct result. In the limit $U/t \rightarrow 0$, the $c0, \iota', \iota''$ branch lines disappear, all spectral weight being transferred over to the $s1$ branch line, which becomes the non-interacting one-electron-removal spectrum. As the limits $U/t \rightarrow 0$ and $U/t \rightarrow \infty$ are approached, the exponent (29) tends to the following values:

$$\begin{aligned} &\zeta_{c0,\iota',\iota''}(q) = \frac{(\iota' - \iota'')^2}{2}; \qquad U/t \rightarrow 0; \\ &\zeta_{c0,\iota',\iota''}(q) = -\frac{\iota'\iota''}{2} + \frac{1}{8}; \qquad U/t \rightarrow \infty, \end{aligned} \tag{32}$$

for the q and k values of the spectral-function expression (28). Thus, in the limit $U/t \rightarrow 0$, it is given by 0 for the branch lines such that $\iota'\iota'' = 1$ and 2 for the branch lines such that $\iota'\iota'' = -1$. Furthermore, for $U/t \rightarrow \infty$ the exponent is given by $-3/8$ for the branch lines such that $\iota'\iota'' = 1$ and $5/8$ for the branch lines such that $\iota'\iota'' = -1$.

Hence, the one-electron-removal $s1$ branch line becomes the non-interacting removal electronic spectrum, which corresponds to $-k_{\rm F} < k < k_{\rm F}$. In turn, for finite values of U/t the spectral weight spreads over a larger two-dimensional region of the (k, ω)-plane. However, most of the spectral weight is located in the vicinity of separated and independent $c0$ and

$s1$ branch lines and of the weak border line mentioned in section 5. Our study provides the momentum and energy dependence of the weight distribution in the vicinity of such $\alpha\nu$ branch lines. In the $m \to 0$ limit, the maximum spread of the one-electron spectral-weight distribution occurs for $U/t \to \infty$, where the problem had already been studied in [20, 21]. The $U/t \to \infty$ maximum spreading of the one-electron-removal spectral weight at electronic density $n = 1/2$ is illustrated in figure 1 of [20] for the spectral function $B(k, \omega)$. Our $U/t \to \infty$ expressions of equations (30) and (32) agree with the results obtained by the method of [20, 21], as mentioned above.

5. Discussion about the relation to the photoemission dispersions of TTF-TCNQ and concluding remarks

An interesting realization of a quasi-1D metal is the organic charge-transfer salt TTF-TCNQ [2–4]. The experimental dispersions in the electron removal spectrum of this quasi-1D conductor as measured by ARPES are shown in figure 9(b) of [3] and figure 4 of [30]. The experimental data in these figures were taken with He I radiation (21.2 eV) at a sample temperature of 60 K on a clean surface obtained by *in situ* cleavage of a single crystal. Instrumental energy and momentum resolution amounted to 70 meV and 0.07 Å^{-1}, respectively.

We note that the low-energy spectral properties of TTF-TCNQ involve inter-chain hopping and electron–phonon interactions. Thus, the 1D Hubbard model PDT results are to be applied above the energies of these processes. The singular branch lines studied in section 4 correspond to the (k, ω)-plane region which contains all the singular features of the one-electron-removal spectral-weight. In spite of the recent improvements in the resolution of photoemission experiments [3–5], it is difficult to measure the exponents and the finest details of the electronic structure experimentally. According to the studies of [37], this is in part due to the extrinsic losses that occur on very anisotropic conducting solids. In turn, the analysis of the problem of [38] presents a number of arguments, both theoretical and experimental, that seem to demonstrate that energy-loss processes occurring once the electron is outside the solid contribute only weakly to the spectrum, and can in most cases be either neglected or treated as a weak structureless background. However, independently of the role of the extrinsic losses, it is difficult to measure the exponents which control the singular features experimentally. Thus, a crucial test for the suitability of the model (1) to describe real quasi-1D materials is whether the ARPES peak dispersions correspond to the singular branch lines and other divergent spectral features predicted by the PDT of [26].

The electronic density of TCNQ is $n = 0.59 < 1$. For densities in the domain $0 < n < 1$ and one-electron removal, the main singular spectral features predicted by the general PDT are of branch-line type. Thus, for TCNQ the main divergent spectral features correspond to the singular branch lines studied in section 4. The only other singular feature is quite weak and corresponds to the lowest line of figure 1 of [30]. In the vicinity of such a border line the spectral-weight distribution corresponds to the power-law dependence (6), which is controlled by a U/t-independent exponent. Due to its weakness such a border line does not lead to any pre-eminent TCNQ spectral feature.

While the theoretical weight-distribution branch-line expressions provided in section 4 refer to all values of U/t and n, a detailed study of the spectral-function k, ω and U/t dependence in the vicinity of the branch lines obtained in this paper confirms the validity of the preliminary predictions of [3, 30]: the electron removal spectrum calculated for $t = 0.4$ eV, $U = 1.96$ eV ($U/t = 4.90$), and $n = 0.59$ yields an almost perfect agreement with the three

TCNQ experimental dispersions. The exception is the low-energy behaviour, as a result of the inter-chain hopping and electron–phonon interactions, as mentioned above. If accounted for a renormalization of the transfer integral due to a possible surface relaxation [3], these values are in good agreement with estimates from other experiments [1, 5].

The experimental TCNQ finite-energy peak dispersions of figure 4 of [30] correspond to the spin $s \equiv s1$ branch line (18) and charge $c \equiv c0, +1, +1$ and $c' \equiv c0, -1, -1$ branch lines (26) of figure 1 of that reference. Those are the main finite-weight singular branch lines in the one-electron-removal spectral function for $U/t = 4.90$ and $n = 0.59$. Importantly, only these main singular features, whose line shape is controlled by negative exponents, lead to TCNQ peak dispersions in the real experiment. The exponent (21) corresponds to the spin $s \equiv s1$ branch line and is plotted in figure 1 for $0 < k < k_F$. The exponents (29) that correspond to the charge $c \equiv c0, +1, +1$ branch line and charge $c' \equiv c0, -1, -1$ branch line are plotted in figures 2 and 3, respectively. As reported in section 4, for finite values of U/t the value of the constant $C_{c0,-1,-1}(q)$ of the spectral-function expression (28) strongly decreases for momentum values such that $2k_F < k < 3k_F$. This is consistent with the absence of TCNQ experimental spectral features for momentum values $k > 0.59\pi \approx 0.50$ Å^{-1} in figure 4 of [30], along the corresponding $c' \equiv c0, -1, -1$ branch line of figure 1 of that reference.

Thus, our detailed branch-line PDT analysis fully agrees with the preliminary theoretical results of [3, 30] for the TCNQ problem. On the other hand, the theoretical predictions for the TTF dispersions presented in [30] are very preliminary. For the electronic density value corresponding to the TCNQ stacks the main singular spectral features are of branch-line type and the only existing border line is quite weak. In contrast, a careful analysis of the problem by means of the general PDT reveals that for the electronic density suitable for the TTF stacks the main singular features are of both branch-line and border-line type. Once the preliminary studies of TTF presented in [30] involve the singular branch-line features only, a very small value of U/t is predicted. However, if instead one takes into account all singular features provided by the PDT, the best quantitative agreement with the TTF experimental dispersions is reached for larger values of U/t, as confirmed elsewhere.

In this paper we have used the exact PDT of [26] to study the energy and momentum dependence of the one-electron-removal spectral-weight distribution in the vicinity of the singular and edge branch lines of the 1D Hubbard model. A careful and detailed analysis of the spectral function expressions in the proximity of the charge and spin branch lines obtained here confirms the validity of the preliminary theoretical predictions of [3, 30], in which the description of the band TCNQ dispersions observed by ARPES in the quasi-1D organic compound TTF-TCNQ is given. The TCNQ conduction band displays spectroscopic signatures of spin-charge separation on an energy scale of the band width. This seems to indicate that the dominant non-perturbative many-electron microscopic processes studied in [26] by means of the PDT and the associated scattering mechanisms investigated in [28] control the unusual finite-energy spectral properties of TTF-TCNQ. The quantitative agreement for the whole finite-energy band width between the theoretically predicted 1D Hubbard model PDT spectral features and the TCNQ photoemission dispersions of TTF-TCNQ reveals that for finite energy the local effects of the Coulomb electronic correlations fully control the spectral properties of that material. Thus, we expect that the long-range Coulomb interactions, disorder and impurity effects play very little part in the finite-energy and/or finite-temperature properties of TTF-TCNQ. That disorder and impurities do not play a major role is confirmed by the occurrence of spin-charge separation for the whole energy band width. Indeed, the presence of disorder and impurities would prevent the separation of the one-electron spectral-weight distribution in terms of spin and charge singular spectral features.

Our present finite-energy description goes beyond the usual TLL low-energy investigations by means of bosonization [10] and conformal-field theory [16]. For low energy the present quantum problem is a TLL. This concept only applies to the parts of the one-electron spectrum of figure 1 of [30] where the spectral dispersions can be linearized. From analysis of the figure branch lines one finds that such a regimen corresponds to low energies. However, our results refer to all values of the group velocities associated with the branch lines plotted in that figure. Thus, the spin-charge separation found here corresponds to the whole finite-energy band width. Only our finite-energy theoretical spectral features describe the experimental photoemission TCNQ dispersions of TTF-TCNQ, once the low-energy phase of TTF-TCNQ is not metallic and corresponds instead to a broken-symmetry state [2]. It follows that for the present TCNQ photoemission problem, the 1D physics described by the 1D Hubbard model only becomes experimentally relevant for finite energy, where the low-energy TLL description does not apply.

A detailed theoretical study of the the TTF experimental dispersions by means of the PDT, including consideration of both singular branch lines studied here and singular border lines is in progress and will be presented elsewhere. Moreover, the calculation of the one-electron spectral function of the 1D Hubbard model for all values of k and ω by use of the general PDT, which consider all contributing processes, is also in progress.

Acknowledgments

We thank A Bjelis, D Bozi, A Castro Neto, F Guinea, E Jeckelmann, P A Lee, J M B Lopes dos Santos, L M Martelo, J P Pouget and U Schwingenschlögl for discussions. JMPC, KP and PDS are grateful for the support of the ESF Science Programme INSTANS 2005-2010, JMPC and PDS for that of the FCT grant POCTI/FIS/58133/2004, JMPC for the hospitality and support of MIT where part of this research was fulfilled and the support of the Calouste Gulbenkian Foundation and Fulbright Commission, KP for that of the OTKA grant T049607, and RC for the support of the Deutsche Forschungsgemeinschaft (CL 124/3-3).

References

[1] Kagoshima S, Nagasawa H and Sambongi T 1987 *One-Dimensional Conductors* (Berlin: Springer) and references therein
[2] Basista H, Bonn D A, Timusk T, Voit J, Jérome D and Bechgaard K 1990 *Phys. Rev.* B **42** 4088
Carmelo J M P, Horsch P, Campbell D K and Castro Neto A H 1993 *Phys. Rev.* B **48** 4200
[3] Sing M, Schwingenschlögl U, Claessen R, Blaha P, Carmelo J M P, Martelo L M, Sacramento P D, Dressel M and Jacobsen C S 2003 *Phys. Rev.* B **68** 125111
[4] Claessen R, Sing M, Schwingenschlögl U, Blaha P, Dressel M and Jacobsen C S 2002 *Phys. Rev. Lett.* **88** 096402
[5] Zwick F, Jérome D, Margaritondo G, Onellion M, Voit J and Grioni M 1998 *Phys. Rev. Lett.* **81** 2974
[6] Lieb Elliott H and Wu F Y 1968 *Phys. Rev. Lett.* **20** 1445
[7] Takahashi M 1972 *Prog. Theor. Phys.* **47** 69
Carmelo J M P and Peres N M R 1997 *Phys. Rev.* B **56** 3717
[8] Peres N M R, Carmelo J M P, Campbell D K and Sandvik A W 1997 *Z. Phys.* B **103** 217
Carmelo J M P C, Peres N M R and Sacramento P D 2000 *Phys. Rev. Lett.* **84** 4673
Baeriswyl D, Carmelo J and Maki K 1987 *Synth. Met.* **21** 271
[9] Simons B D, Lee P A and Altshuler B L 1993 *Phys. Rev. Lett.* **70** 4122
Arikawa M, Saiga Y and Kuramoto Y 2001 *Phys. Rev. Lett.* **86** 3096
Penc K and Shastry B S 2002 *Phys. Rev.* B **65** 155110
[10] Schulz H J 1990 *Phys. Rev. Lett.* **64** 2831
Carmelo J M P, Castro Neto A H and Campbell D K 1994 *Phys. Rev. Lett.* **73** 926
Carmelo J M P, Castro Neto A H and Campbell D K 1995 *Phys. Rev. Lett.* **74** 3089 (erratum)
Carmelo J M P, Castro Neto A H and Campbell D K 1994 *Phys. Rev.* B **50** 3683
[11] Woynarovivh F 1989 *J. Phys. A: Math. Gen.* **22** 4243

[12] Ogata M and Shiba H 1990 *Phys. Rev.* B **41** 2326
[13] Kawakami N and Yang S K 1990 *Phys. Lett.* A **148** 359
[14] Frahm H and Korepin V E 1990 *Phys. Rev.* B **42** 10 553
[15] Brech M, Voit J and Buttner H 1990 *Europhys. Lett.* **12** 289
[16] Frahm H and Korepin V E 1991 *Phys. Rev.* B **43** 5653
[17] Ogata M, Sugiyama T and Shiba H 1991 *Phys. Rev.* B **43** 8401
[18] Penc K and Sólyom J 1993 *Phys. Rev.* B **47** 6273
[19] Carmelo J M P and Castro Neto A H 1993 *Phys. Rev. Lett.* **70** 1904
Carmelo J M P, Castro Neto A H and Campbell D K 1994 *Phys. Rev.* B **50** 3667
[20] Penc K, Hallberg K, Mila F and Shiba H 1996 *Phys. Rev. Lett.* **77** 1390
[21] Penc K, Hallberg K, Mila F and Shiba H 1997 *Phys. Rev.* B **55** 15475
[22] Sorella S and Parola A 1996 *Phys. Rev. Lett.* **76** 4604
[23] Sénéchal D, Perez D and Pioro-Ladrière M 2000 *Phys. Rev. Lett.* **84** 522
[24] Carmelo J M P, Román J M and Penc K 2004 *Nucl. Phys.* B **683** 387
[25] Carmelo J M P and Sacramento P D 2003 *Phys. Rev.* B **68** 085104
[26] Carmelo J M P, Penc K and Bozi D 2005 *Nucl. Phys.* B **725** 421
Carmelo J M P, Penc K and Bozi D 2006 *Nucl. Phys.* B **737** 351 (erratum)
Carmelo J M P and Penc K 2006 *Eur. Phys. J.* B at press (*Preprint* cond-mat/0311075)
[27] Carmelo J M P and Penc K 2006 *Phys. Rev.* B **73** 113112
Carmelo J M P, Martelo L M and Penc K 2006 *Nucl. Phys.* B **737** 237
[28] Carmelo J M P 2005 *J. Phys.: Condens. Matter* **17** 5517
[29] Carmelo J M P, Bozi D and Sacramento P D 2006 *Preprint* cond-mat/0603665
Carmelo J M P, Hibberd K E and Andrei N 2006 *Preprint* cond-mat/0603446
[30] Carmelo J M P C, Penc K, Martelo L M, Sacramento P D, Lopes dos Santos J M B, Claessen R, Sing M and Schwingenschlögl U 2004 *Europhys. Lett.* **67** 233
[31] Benthien H, Gebhard F and Jeckelmann E 2004 *Phys. Rev. Lett.* **92** 256401
[32] Carmelo J M P, Guinea F, Penc K and Sacramento P D 2004 *Europhys. Lett.* **68** 839
[33] Bares P A, Carmelo J M P, Ferrer J and Horsch P 1992 *Phys. Rev.* B **46** 14624
[34] Meden V and Schönhammer K 1992 *Phys. Rev.* B **46** 15753
[35] Voit J 1993 *Phys. Rev.* B **47** 6740
Voit J 1993 *J. Phys.: Condens. Matter* **5** 8305
[36] Schönhammer K and Meden V 1993 *Phys. Rev.* B **47** 16205
[37] Joynt R 2000 *Science* **284** 777
[38] Schulte K, James M A, Steeneken P G, Sawatzky G A, Suryanarayanan R, Dhalenne G and Revcolevschi A 2001 *Phys. Rev.* B **63** 165429